Comparative NMR Study of A_n-Bulge Loops in DNA Duplexes: Intrahelical Stacking of A, A-A, and A-A-A Bulge Loops†

Mark A. Rosen,‡ David Live,§ and Dinshaw J. Patel*,‡

Department of Biochemistry and Molecular Biophysics, College of Physicians and Surgeons, Columbia University, New York, New York 10032, and Chemistry Department, California Institute of Technology, Pasadena, California 91125

Received December 16, 1991

ABSTRACT: We have prepared a series of deoxyoligonucleotide duplexes of the sequence d(G-C-A-T-C-G-X-G-C-T-A-C-G)·d(C-G-T-A-G-C-C-G-A-T-G-C), in which X represents either one (A), two (A-A), or three (A-A-A) unpaired adenine bases. Using two-dimensional proton and phosphorus NMR spectroscopy, we have characterized conformational features of these bulge–loop duplexes in solution. We find that Watson–Crick hydrogen bonding is intact for all 12 base pairs, including the GC bases that flank the bulge loop. Observation of NOE connectivities in both H_2O and D_2O allows us to unambiguously localize all of the bulged adenine residues to intrahelical positions within the duplex. This is in contrast to an earlier model for multiple-base bulge loops in DNA [Bhattacharyya, A., & Lilley, D. M. J. (1989) *Nucleic Acids Res. 17*, 6821–6840], in which all but the most 5′ bulged base are looped out into solution. We find that insertion of two or three bases into the duplex results in the disruption of specific sequential NOEs for the base step across from the bulge loop site on the opposite strand. This disruption is characterized by a partial shearing apart of these bases, such that certain sequential NOEs for this base step are preserved. We observe a downfield-shifted phosphorus resonance, which we assign in the A-A-A bulge duplex to the 3′ side of the last bulged adenine residue. Proton and phosphorus chemical shift trends within the A_n-bulge duplex series indicate that there is an additive effect on the structural perturbations caused by additional unpaired bases within the bulge loop. This finding parallels previous observations [Bhattacharyya, A., & Lilley, D. M. J. (1989) Nucleic Acids Res. 17, 6821–6840; Hsieh, C.-H., & Griffith, J. D. (1989) *Proc. Natl. Acad. Sci. U.S.A. 86*, 4833–4837] on the magnitude of the induced bending of DNA duplexes by multiple-base bulge loops.

Extrahelical bases, or "bulges", are thought to play an important role in nucleic acid structure and function. They are the proposed intermediates in the generation of frame-shift mutations when errors in DNA replication occur (Streisinger et al., 1966). Certain intercalative mutagens have been found to bind with an increased affinity at or near bulge sites in DNA (Nelson & Tinoco, 1985; White & Draper, 1987), suggesting that these ligands could stabilize bulged DNA structures during or after DNA replication. Another important role for extrahelical bases may be in large RNA molecules, such as ribosomal RNA, where bulges are often predicted to occur in the secondary structure (Gutell & Fox, 1988; Wolters & Erdmann, 1988). It has been postulated that extrahelical bases might mediate protein–nucleic acid interactions, either by contacting protein residues directly or by producing a distinct tertiary structure to which the protein binds (Peattie et al., 1981; Romaniuk et al., 1987). A report on the recognition of TAR RNA from HIV-1 by carboxy-terminal fragments of Tat protein (Weeks et al., 1990) demonstrated the pivotal role of a trinucleotide bulge within the folded RNA molecule. Clearly, elucidation of the structure of extrahelical bases within DNA and RNA duplexes would be of great help in furthering our understanding of the role they play in the biology of the cell.

The solution conformation of a single bulged base within an oligomeric DNA or RNA duplex has been studied by NMR for a variety of sequences and extrahelical bases. The observations from these studies demonstrate that, in general, bulged purines will stack into the duplex (Patel et al., 1982; Hare et al., 1986; Roy et al., 1987; Woodson & Crothers, 1988; Kalnik et al., 1989a; Nikonowicz et al., 1989, 1990), whereas bulged pyrimidines may be either stacked in or looped out into solution, depending upon the temperature and the flanking sequence (Morden et al., 1983, 1990; van den Hoogen et al., 1988a,b; Kalnik et al., 1989b, 1990).

X-ray crystallography has also been used in an effort to determine the conformation of a single extrahelical base within DNA. Two sequences, a tridecamer (Joshua-Tor et al., 1988) and a pentadecamer (Miller et al., 1988), each with adenine as the extra base, have been crystalized. The early analysis in both cases suggested that an extrahelical adenine was looped out from the double helix. However, in the case of the tridecamer, more recent analysis has established that one of the two symmetrically related adenines loops out from the helix while the second remains stacked within the molecule (Joshua-Tor et al., 1992). In this structure, the looped-out base forms a Hoogsteen pair with the stacked-in adenine of an adjacent duplex. This result emphasizes the role packing forces can play in determining the conformation of extrahelical bases in the crystalline state.

DNA duplexes containing a bulged base exhibit abnormally slow migration on polyacrylamide gels (Rice & Crothers, 1988), suggesting that the DNA is bent by the unpaired base. Similar results have been obtained for bulged bases within double-stranded RNA and DNA·RNA hybrid duplexes (Bhattacharyya et al., 1990). The amount of bending caused by one unpaired base has been shown to depend on the identity of both the bulged base and the flanking sequence (Wang &

† This research was supported by NIH Grant GM34504 to D.P. M.R. was supported by NIH MSTP Training Grant 5-T32-GM07376. The NMR spectrometers were purchased from funds donated by the Robert Woods Johnson Trust toward setting up an NMR center in the Basic Medical Sciences at Columbia University.

* Author to whom correspondence should be addressed.
‡ Columbia University.
§ California Institute of Technology.

0006-2960/92/0431-4004$03.00/0

Chart I

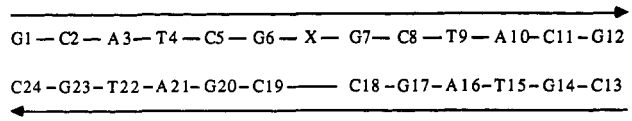

X	
---	Control Duplex
Ax	A1-bulge Duplex
Ax-Ay	A2-bulge Duplex
Ax-Ay-Az	A3-bulge Duplex
Ax-Iy-Az	AIA-bulge Duplex
Ax-Ty-Az	ATA-bulge Duplex

Griffith, 1990). Gel mobility and electron microscopy studies have been undertaken as well on DNA or RNA duplexes that contain bulge loops with two or more bases (Hsieh & Griffith, 1989; Bhattacharyya & Lilley, 1989; Tang & Draper, 1990). In these studies it was shown that, for bulge loops up to seven bases long, as the number of bases within the bulge loop increased, so did the magnitude of the induced bend in the helical axis.

Since multiple-base bulge loops have been shown to cause significant bending in DNA duplexes, with presumably restricted flexibility in solution, we felt that they would be ideal for study by NMR spectroscopy. We have therefore prepared a series of oligomeric DNA duplexes containing a centrally placed bulge loop whose size and sequence varies. The sequence and numbering scheme used throughout are shown in Chart I. In our sequence, the bulge loop is flanked by GC base pairs in order to increase the duplex stability near the bulge loop site. We have also made our bulge loops purine-rich so as to increase the possibility of favorable stacking interactions among the bases within the bulge loop and the neighboring guanine residues.

In this paper we examine the solution NMR results for the series of A_n-bulge duplexes (where n varies from 0 to 3). We focus our analysis on the A-A bulge (designated A_2-bulge) and the A-A-A bulge (designated A_3-bulge) duplexes, as these are the first multiple-base bulge loops in DNA to be studied by NMR spectroscopy. In the following paper in this issue, we present more quantitative results for a sequence variant of the A_3-bulge duplex containing an A-T-A bulge loop.

Materials and Methods

Synthesis and Purification of DNA Oligomers. DNA oligomers were synthesized on the 10-μmol scale using a Beckman System One Plus automated DNA synthesizer employing standard phosphoramidite chemistry on solid supports. The oligomers were purified by reversed-phase HPLC using preparative C-4 columns (Rainin) and were desalted by gel filtration through Sephadex G-25 columns (Pharmacia). Purity was judged by analytical HPLC using a C-18 column (Waters) and was greater than 97% in all cases.

Preparation of NMR Samples. Equimolar duplexes were formed via successive additions of one strand to its complementary partner in unbuffered D_2O and observation of the NMR resonances of base and methyl protons at high temperature. The correct stoichiometry was determined by comparing integrated areas of resolved resonance lines corresponding to equivalent protons on opposite strands. Upon successful titration, an aliquot of concentrated buffer solution was added. Following lyophilization, the samples were dissolved in 0.4 mL of deionized H_2O, for a DNA concentration of approximately 3 mM per strand. Final buffer conditions were 10 mM sodium phosphate, with 100 mM NaCl and 0.2 mM EDTA. The pH was corrected to 6.5, following which the samples were relyophilized to dryness. For experiments in H_2O, oligomers were dissolved in 0.4 mL of deionized H_2O containing 10% D_2O. For experiments in D_2O, oligomers were lyophilized repeatedly in 99% D_2O and were finally dissolved in 0.4 mL of 99.96% D_2O prior to two-dimensional spectroscopy. The uncorrected pH readings in D_2O were 6.8.

Proton NMR Spectroscopy. One- and two-dimensional proton NMR spectra were recorded on Bruker AM-400 and AM-500 spectrometers. Spectra in H_2O were acquired with a jump-and-return pulse sequence (Plateau & Gueron, 1982) to suppress the solvent signal. Those in D_2O were recorded with a low-power preirradiation of the residual HDO signal during the recovery period. All spectra were referenced relative to an external 3-trimethylsilyl(*2,2,3,3-d*$_4$)proprionate (TSP) standard. Phase-sensitive NOESY experiments (States et al., 1982) in H_2O were acquired with 70° preparation and mixing pulses, followed by a jump-and-return reading pulse. Typically, 160 scans of 1024 complex points in a 25 ppm spectral width were acquired for each of the 256 real and imaginary t_1 increments. NOESY experiments in D_2O were recorded with a 10 ppm spectral width consisting of 64 scans per t_1 increment and a 1.5-s relaxation delay. Two-dimensional data sets were apodized with a 30° shifted sine bell window function in both dimensions and zero-filled in the t_1 dimension to give a two-dimensional square matrix of 1024 points. Magnitude COSY experiments were acquired in a similar manner to the NOESY spectra, but with 512 t_1 increments. They were multiplied by an unshifted sine bell in each dimension and presented in the magnitude mode subsequent to Fourier transformation in the t_1 dimension. All two-dimensional data sets were processed on a Vax 11/780 computer using the FTNMR software package (D. Hare, Hare Research, Inc.). Difference one-dimensional NOE experiments were performed by acquiring FIDs with a 0.2–0.4-s preirradiation of the peak of interest. Alternate FIDs were recorded with the saturation on or off resonance in 32 scan increments to correct for magnetic field drift during the experiment. The control FID was then subtracted from the experimental, with 5.0-Hz line broadening prior to Fourier transformation.

Phosphorus NMR Spectroscopy. One-dimensional, proton-decoupled, phosphorus spectra were recorded on a Bruker AM-300 spectrometer (phosphorus frequency, 121.5 MHz) with Waltz decoupling during acquisition. Two-dimensional, proton-detected, phase-sensitive ^{31}P–^1H correlation experiments were performed on a General Electric GN-500 spectrometer. The pulse sequence used was as described previously (Sklenar et al., 1986) with a modification in the phase cycle (Sklenar & Bax, 1987). Two-dimensional data sets were collected with 256 scans for each of 128 t_1 increments. The spectral widths were 2000 Hz in 1024 points for protons and 1000 Hz in 128 points (zero filled to 512 points) for phosphorus. The data were processed on a Nicolet 1280 computer using the spectrometer software provided. Proton and phosphorus chemical shifts were referenced relative to TSP and trimethyl phosphate (TMP), respectively, as described previously (Live et al., 1984).

Results

Comparison of Exchangeable Proton Spectra. The downfield portions of the one-dimensional proton NMR spectra for the control duplex and the three A_n-bulge duplexes in H_2O

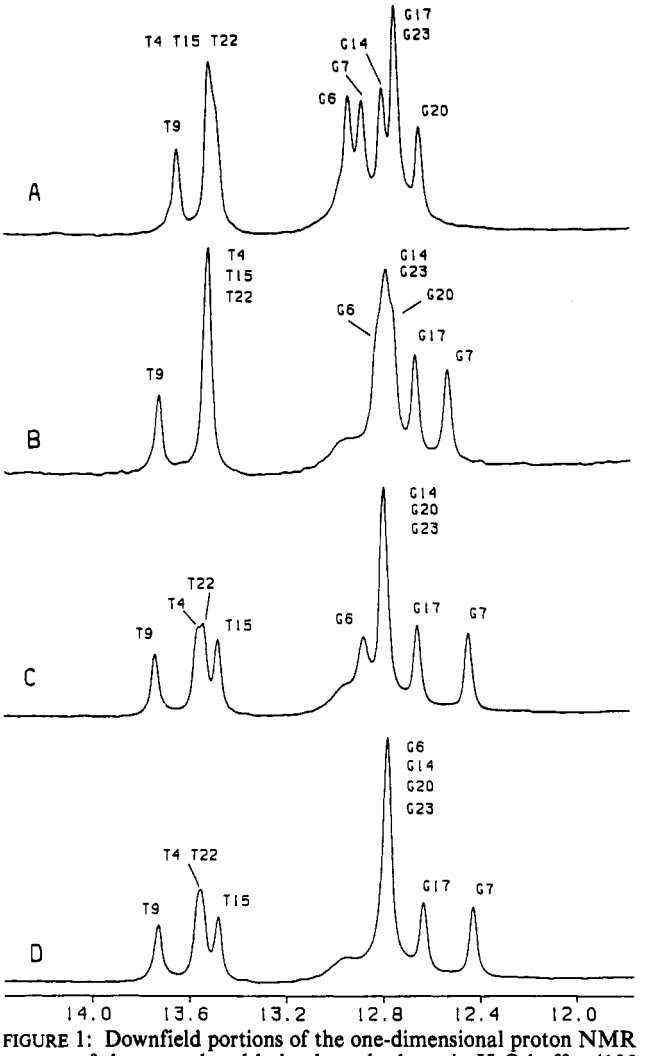

FIGURE 1: Downfield portions of the one-dimensional proton NMR spectra of the control and bulge loop duplexes in H_2O buffer (100 mM NaCl, 10 mM sodium phosphate, 0.2 mM EDTA), pH 6.5, at 25 °C. (A) Control duplex; (B) A_1-bulge duplex; (C) A_2-bulge duplex; (D) A_3-bulge duplex. Imino proton assignments are shown in the figure and are discussed in the text.

buffer, pH 6.5, at 25 °C, are shown in Figure 1. Imino proton assignments are included in the figure. Thymine imino protons were assigned on the basis of the observation of a strong NOE to the nonexchangeable H2 proton from the adenine residue with which it forms a Watson–Crick hydrogen-bonded pair. These latter protons were assigned on the basis of characteristic intra- and intermolecular NOEs seen in NOESY spectra in D_2O. Guanine imino protons were assigned on the basis of observable NOEs to the amino protons (hydrogen-bound and exposed) of the partner cytosine residue. These geminal amino protons were first assigned on the basis of the NOEs to each other and to the nonexchangeable cytosine H5 protons, whose assignments had been previously determined via NOESY experiments in D_2O. As is seen in the labeling of the imino proton resonances in Figure 1, for each of the duplexes studied, we could locate the imino protons of both G6 and G7 between 12.0 and 13.0 ppm. Imino protons that do not participate in base pairing in DNA resonate between 10.0 and 11.0 ppm. The downfield location of the G6 and G7 imino protons establishes that, in each duplex, the G6·C19 and G7·C18 Watson–Crick base pairs form under the conditions studied, even in the presence of a three-base bulge loop.

Upon inspection of the four spectra in Figure 1, one observes that the pattern of imino resonances for the A_1-bulge duplex differs considerably from that of the control duplex. In particular, the imino protons of G6 and G7 move upfield by 0.10 and 0.34 ppm, respectively. Other resonances move downfield, indicating that the changes seen are caused, at least in part, by conformational differences between the two molecules and are not simply a result of an increase in the rate of solvent exchange due to the lower stability of the bulge-containing duplex. In contrast, the differences between the spectra of the A_1-bulge duplex and those of the A_2-bulge and A_3-bulge duplexes are more qualitative in nature. This suggests that the structural differences between these three molecules are more subtle than are the differences between the control and the A_1-bulge duplexes.

We expected that a single-bulged adenine located between two guanines would adopt an "intrahelical" conformation by stacking into the double helix. This is the result that had been previously obtained for a bulged adenine residue within a similar sequence context (Kalnik et al., 1989a). Using one-dimensional difference NOE experiments, we observed NOEs from the H2 proton of Ax to the imino protons of both G6 and G7. This result confirms that the bulged adenine in the A_1-bulge duplex stacks into the helix and that the differences between the spectra shown in Figure 1A,B are due to the insertion of an unpaired adenine residue between the bases G6 and G7 in the A_1-bulge duplex. By contrast, the qualitative resemblance among the three spectra in Figure 1B,C,D suggests that these bulge loop duplexes share certain conformational features.

Chemical Shift Assignments for the Control and A_1-Bulge Duplexes. The procedure used to assign the solvent-labile imino and cytosine amino protons has been described above. The nonexchangeable base and sugar proton resonances were assigned via standard methods using two-dimensional through-bond (COSY) and through-space (NOESY) NMR experiments (Hare et al., 1983; Wüthrich, 1986). Since each sugar ring exists as an isolated spin system, COSY experiments provide information regarding the identity of sugar protons belonging to the same residue. Sequential assignments are then made on the basis of the pattern of intra- and interresidue distance connectivities seen in NOESY experiments. In right-handed double helices, the base proton (H8 or H6) will show an NOE to the H1′ proton of the same residue, as well as to the H1′ proton of the preceding residue in the 5′ direction. Due to the efficiency of spin diffusion among protons within the deoxyribose ring, sequential NOEs are also seen involving the H2′, H2″, and (at longer mixing times) H3′ protons. Base to base NOEs also allow unambiguous assignments for right-handed DNA. For an N–Y base step (5′ to 3′ direction), where N is any nucleotide and Y is a pyrimidine, there will be a strong NOE from the base proton (H8 or H6) of the first base to the H5 proton (for cytosines) or the CH_3 protons (for thymines) of the second base.

We analyzed the two-dimensional NMR spectra of the control and A_1-bulge duplexes in both H_2O and D_2O buffer. Representative contour plots of the base to H1′ regions of the NOESY experiments in D_2O buffer at 25 °C are shown in Figure S1 for the control duplex and in Figure S2 for the A_1-bulge duplex (Supplementary Material). The chemical shift assignments for the control duplex are listed in Tables S-I and S-II; those for the A_1-bulge duplex are listed in Tables S-III and S-IV (Supplementary Material). Both of these duplexes exhibited spectra indicative of B-type DNA. No unusual NOEs were observed that might suggest a nonstandard conformation. Proton assignments and NOESY results for the A_1-bulge duplex were consistent with the adenine adopting a stacked-in conformation. NOE cross peak intensity

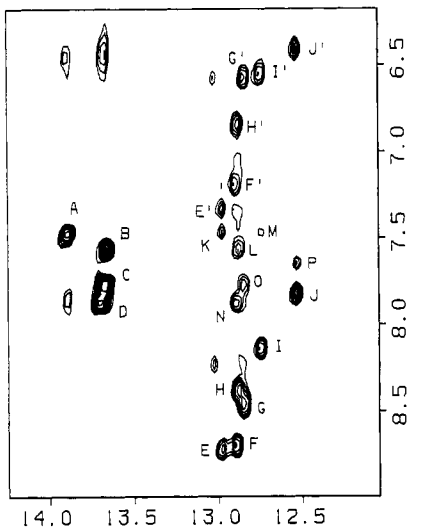

FIGURE 2: Expanded contour plot of the NOESY experiment (150-ms mixing time) on the A_2-bulge duplex in H_2O buffer at 0 °C. Assignments for labeled cross peaks are as follows: (A) T9(imino)–A16(H2); (B) T15(imino)–A10(H2); (C) T22(imino)–A3(H2); (D) T4(imino)–A21(H2); (E,E′) G6(imino)–C19(amino, b/e); (F,F′) G20(imino)–C5(amino, b/e); (G,G′) G23(imino)–C2(amino, b/e); (H,H′) G14(imino)–C11(amino, b/e); (I,I′) G17(imino)–C8(amino, b/e); (J,J′) G7(imino)–C18(amino, b/e); (K) G6(imino)–Ax(H2); (L) G14(imino)–A10(H2); (M) G17(imino)–A16(H2); (N) G20-(imino)–A21(H2); (O) G23(imino)–A3(H2); (P) G7(imino)–Ay(H2). The symbols "b" and "e" refer to the hydrogen-bonded and exposed cytosine amino protons. Cross peaks E,E′ and J,J′ demonstrate intact base pairing of the G6·C19 and the G7·C18 Watson–Crick base pairs, respectively. Cross peaks K and P localize the bulged residues Ax and Ay as stacked with their respective flanking GC base pairs.

and chemical shift trends were similar to those previously reported for a single-bulged adenine located between two guanine residues (Kalnik et al., 1989a).

Exchangeable Protons in the A_2-Bulge Duplex. An expanded contour plot of the NOESY experiment (150-ms mixing time) for the A_2-bulge duplex in H_2O buffer at 0 °C is shown in Figure 2. The horizontal axis contains the chemical shifts of the imino protons while the vertical axis contains the shifts for the base and amino protons. Cross peaks A–D in the figure represent NOEs from each of the four thymine imino protons to the adenine H2 proton within the same base pair. Specific assignments are indicated in the caption to the figure. NOE cross peaks between the guanine imino protons and the cytosine amino protons (hydrogen-bonded and exposed) for each of the six nonterminal base pairs are also indicated (peaks E,E′–J,J′). The observation of NOEs from the G6 and G7 imino protons to the C19 (peaks E,E′) and C18 (peaks J,J′) amino protons, respectively, confirms that these bases participate in Watson–Crick pairing despite the destabilizing presence of the adjacent A-A bulge loop. We also see several sequential NOEs between guanine imino protons and adenine H2 protons from neighboring base pairs. These cross peaks are labeled L–O in Figure 2 and are individually identified in the caption. Two remaining cross peaks, labeled K and P, are identified in the figure. These are, respectively, NOEs between the G6(imino) and Ax(H2) protons, and between the G7(imino) and Ay(H2) protons. For NOESY experiments at this mixing time, NOE intensity falls off rapidly at a distance beyond about 4 Å. Therefore, the observation of an NOE from the H2 proton of each of the two bulged adenine residues to the imino proton of each flanking GC base pair unambiguously places both of these adenines in intrahelical positions, stacked within the duplex. The A_2-bulge duplex thus contains not one, but two intrahelically

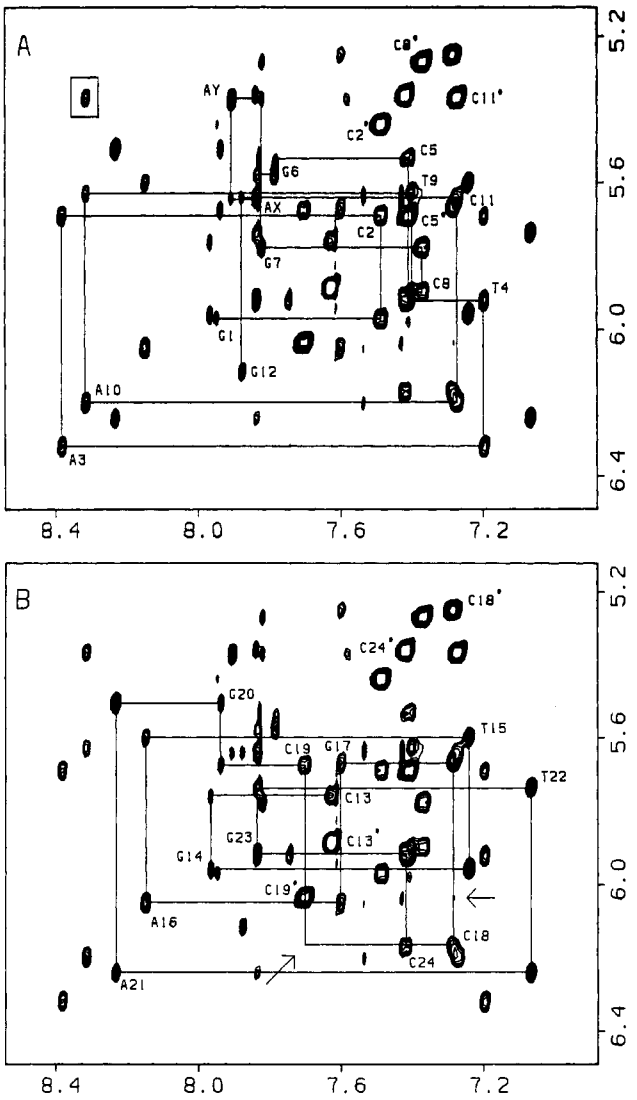

FIGURE 3: Expanded contour plot of the base to H1′ region of the NOESY experiment (250-ms mixing time) on the A_2-bulge duplex in D_2O buffer at 25 °C. Sequential distance connectivities are traced out for the bulge-containing strand (panel A) and partner strand (panel B) separately. Intraresidue base to H1′ cross peaks are labeled by residue. Asterisks indicate the H6–H5 cross peak for cytosine residues. The boxed cross peak in panel A is the A10(H8)–C11(H5) NOE typical for any N–C base step. The arrows in panel B indicate absent or weak NOEs for the C18–C19 base step across from the bulge site.

located bulged bases, demonstrating the ability of the DNA duplex to accommodate adjacent unpaired bases within an otherwise normal double helix. The chemical shifts of all exchangeable and adenine H2 protons assigned in the A_2-bulge duplex are listed in Table I.

Nonexchangeable Protons in the A_2-Bulge Duplex. An expanded contour plot of the base to H1′ region of the NOESY experiment (250-ms mixing time) for the A_2-bulge duplex in D_2O buffer at 25 °C is shown in duplicate in Figure 3. Sequential assignments are traced out with the intraresidue base to H1′ cross peak labeled for each base. For clarity, the assignments for the individual strands are shown separately in panels A and B. For the bulge-containing strand (panel A), we find that it is possible to trace the NOE connectivity pattern throughout the bulge loop site without interruption. That is, we see all NOE connectivities for the sequence: G6(H1′)-Ax(H8)-Ax(H1′)-Ay(H8)-Ay(H1′)-G7(H8). This suggests that the Ax-Ay segment retains a helical conformation as it stacks into the DNA duplex. We note that the chemical shifts of protons from residues Ax and Ay are located further

Table I: Exchangeable and A(H2) Proton Chemical Shifts of the A_2-Bulge Duplex in H_2O Buffer, pH 6.5, at 0 °C

	chemical shifts (ppm)				
base pair	H3	H1	NH_2b^a	NH_2e^b	H2
G1·C24			8.22	6.58	
C2·G23		12.84	8.45	6.58	
A3·T22	13.66				7.76
T4·A21	13.68				7.86
C5·G20		12.89	8.70	7.19	
G6·C19		12.97	8.72	7.33	
Ax					7.47
Ay					7.64
G7·C18		12.53	7.82	6.42	
C8·G17		12.74	8.14	6.55	
T9·A16	13.88				7.47
A10·T15	13.65				7.56
C11·G14		12.87	8.37	6.82	
G12·C13			8.14	7.06	

[a] Hydrogen-bonded cytosine amino protons. [b] Exposed cytosine amino protons.

upfield than are those from corresponding protons on other adenine residues. The effect is most striking for the H1′ proton of Ay, located at 5.37 ppm. This finding is consistent with the intrahelical location of the two bulged bases. Protons located on residues that are "looped out" into solution would be expected to resonate at a more downfield position due to the loss of magnetic shielding from base stacking.

In Figure 3B, we see the sequential connectivities for the partner (bulgeless) strand. Particularly striking in this case is the absence of an NOE between the C18(H1′) and C19(H6) protons, as indicated by the arrow in the lower center of the figure. This discontinuity lies precisely at the base step which flanks the bulge loop site on the opposite strand. We also see an extremely weak connectivity (apparent only at lower contour levels) between the H6 proton of C18 and the H5 proton of C19 (arrow at lower right, Figure 3B). This weak NOE contrasts with the typically strong NOEs seen at other N–Y base steps. For example, the boxed cross peak in the upper left of Figure 3A demonstrates the intensity of the A10-(H8)–C11(H5) NOE. Furthermore, in the control duplex containing no bulge loop, we do see a prominent NOE between the C18(H6) and C19(H5) protons (Figure S1B, Supplementary Material). The absence or weakening of sequential NOEs between C18 and C19 is therefore not due to an alternative conformation within the G-C-C-G sequence. Instead, there must be an increase in the separation between the C18 and C19 bases of the A_2-bulge duplex, consistent with a model in which the bulged residues are inserted into the helix.

The pattern of sequential NOEs seen in the base to H1′ proton region for the A_2-bulge duplex is present in the base to H2′,2″ region as well. Full sequential connectivities are conserved throughout the bulge loop site. The C18–C19 connectivity, absent in the H1′ region, is present in the H2′,2″ region but is quite weak. However, in the base to H3′ region, the C18–C19 sequential connectivity is much stronger. This region of the NOESY spectrum is shown in Figure 4A. The intraresidue H6 to H3′ NOE cross peaks for both C18 and C19 are labeled. The arrow indicates an intense sequential cross peak between C18(H3′) and C19(H6). We also observe a strong C18(H3′) to C19(H5) cross peak in a separate region of the NOESY spectrum, shown in Figure 4B. Since the interresidue H3′ to H6/H8 distance is ordinarily greater than 5.0 Å in B-DNA, sequential NOE connectivities in this region are usually due to spin diffusion. However, the absence of any other strong, sequential NOEs for the C18–C19 base step leads us to conclude that the cross peak seen in Figure 4A is a direct NOE indicative of an unusual backbone conformation at this

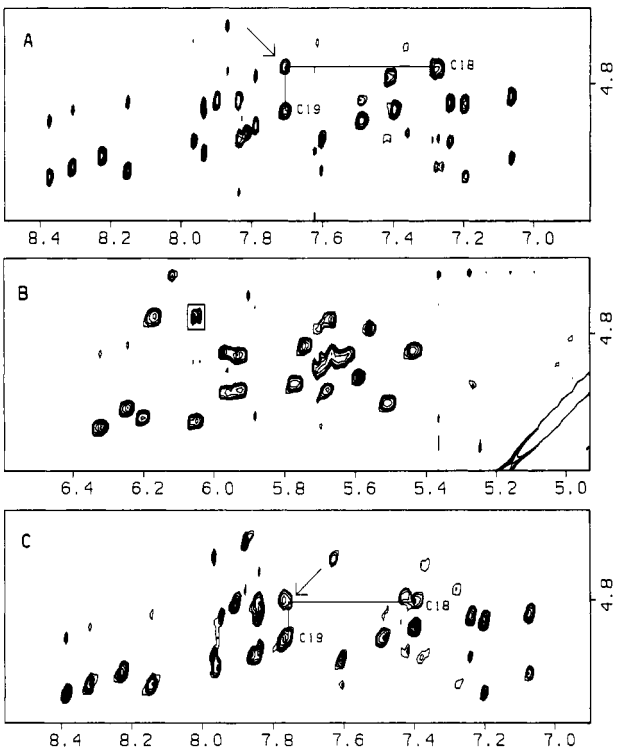

FIGURE 4: Expanded regions of NOESY experiments (250-ms mixing time) on the A_2-bulge and A_3-bulge duplexes in D_2O buffer. (A) Base to H3′ region of the A_2-bulge duplex. The C18 and C19 intraresidue H6–H3′ cross peaks are labeled. The sequential C18(H3′) to C19(H6) cross peak is indicated by the arrow. The experiment was run at 35 °C to allow for observation of the C18(H3′) proton, which falls under the residual HDO resonance at 25 °C. (B) H1′ to H3′ region of the same experiment as in panel A. Cross peak assignment for the boxed peak is C19(H5)–C18(H3′). (C) Base to H3′ region for the A_3-bulge duplex at 25 °C. Once again, C18 and C19 H6–H3′ cross peaks are labeled. The arrow indicates the sequential C18(H3′)–C19(H6) NOE.

site. Evidently, the separation between C18 and C19 is not so large as to preclude the observation of a strong distance connectivity between these two residues via the C18(H3′) proton. We conclude that the separation of the two cytosine residues across from the A-A bulge loop does not result simply from the wedging apart of these two bases along the helical axis, as it is often represented schematically. In addition, there must be some lateral displacement or rotation, so as to increase the overall separation between the two bases while retaining a relatively short C18(H3′) to C19(H6) distance. Table II lists the chemical shifts of all nonexchangeable protons assigned in the A_2-bulge duplex.

Exchangeable Protons in the A_3-Bulge Duplex. We performed a similar set of experiments on the A_3-bulge duplex. In Figure 5, an expanded contour plot of the NOESY experiment (150-ms mixing time) on the A_3-bulge duplex in H_2O buffer at 0 °C is shown. The same region that was plotted in Figure 2 for the A_2-bulge duplex is presented here. Individual cross peaks are identified in the caption to the figure. As was the case for the A_2-bulge duplex, the most upfield imino proton belongs to G7. We observe three cross peaks to this imino proton in the region shown. Once again, two of these peaks (J and J′) belong to the hydrogen-bonded and exposed C18 amino protons. This result demonstrates that the G7·C18 base pair remains intact in the A_3-bulge duplex. A third cross peak to the G7(imino) proton can be seen (peak P), and it is assigned to the H2 proton from the third adenine in the bulge loop, Az. This NOE places Az in an intrahelical position within the duplex, just as we observed for Ay in the A_2-bulge duplex (Figure 2).

Table II: Chemical Shift Assignments for the A_2-Bulge Duplex in D_2O Buffer at 25 °C

	chemical shifts (ppm)							
base	H8/H6	H5/CH_3	H2	H1′	H2′	H2″	H3′	H4′
G1	7.94			5.97	2.62	2.79	4.85	4.24
C2	7.48	5.44		5.69	2.19	2.50	4.90	4.22
A3	8.38		7.74	6.32	2.74	2.99	5.05	4.45
T4	7.20	1.47		5.92	1.99	2.40	4.85	4.16
C5	7.41	5.69		5.53	1.80	2.17		4.02
G6	7.78			5.58	2.33	2.39	4.91	4.18
Ax	7.83		7.43	5.64	2.14	2.23	4.83	4.09
Ay	7.90		7.58	5.37	2.48	2.48	4.84	4.22
G7	7.82			5.78	2.64	2.64	4.94	4.35
C8	7.37	5.27		5.89	2.01	2.40		4.21
T9	7.40	1.63		5.63	2.13	2.44	4.87	4.15
A10	8.31		7.53	6.20	2.71	2.85	5.03	4.42
C11	7.27	5.36		5.64	1.84	2.27		4.14
G12	7.87			6.11	2.56	2.34	4.64	4.15
C13	7.62	5.88		5.76	2.01	2.42	4.69	4.06
G14	7.96			5.96	2.66	2.77	4.96	4.35
T15	7.24	1.48		5.60	2.07	2.38	4.85	4.17
A16	8.15		7.43	6.05	2.69	2.86	5.04	4.40
G17	7.60			5.67	2.44	2.57	4.95	4.34
C18	7.28	5.25		6.16	1.85	2.10		4.26
C19	7.70	6.03		5.68	2.20	2.45	4.87	4.18
G20	7.94			5.50	2.70	2.78	4.99	4.28
A21	8.23		7.83	6.24	2.64	2.91	5.00	4.42
T22	7.06	1.40		5.73	1.93	2.34	4.83	4.12
G23	7.83			5.91	2.57	2.68	4.95	4.34
C24	7.41	5.36		6.17	2.18	2.18	4.48	4.05

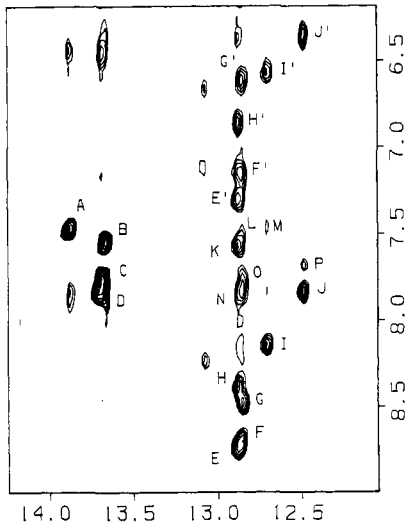

FIGURE 5: Expanded contour plot of the NOESY experiment (150-ms mixing time) on the A_3-bulge duplex in H_2O buffer at 0 °C. Assignments for labeled cross peaks are as follows: (A) T9(imino)–A16(H2); (B) T15(imino)–A10(H2); (C) T22(imino)–A3(H2); (D) T4(imino)–A21(H2); (E,E′) G6(imino)–C19(amino, b/e); (F,F′) G20(imino)–C5(amino, b/e); (G,G′) G23(imino)–C2(amino, b/e); (H,H′) G14(imino)–C11(amino, b/e); (I,I′) G17(imino)–C8(amino, b/e); (J,J′) G7(imino)–C18(amino, b/e); (K) G6(imino)–Ax(H2); (L) G14(imino)–A10(H2); (M) G17(imino)–A16(H2); (N) G20-(imino)–A21(H2); (O) G23(imino)–A3(H2); (P) G7(imino)–Az(H2). The symbols "b" and "e" refer to the hydrogen-bonded and exposed cytosine amino protons. Cross peaks E,E′ and J,J′ demonstrate intact base pairing of the G6·C19 and the G7·C18 Watson–Crick base pairs, respectively. Cross peaks K and P localize the bulged residues Ax and Az as stacked with their respective flanking GC base pairs.

Unfortunately, in the A_3-bulge duplex, the G6 imino proton has moved to a position in which it overlaps with three other guanine imino protons. We can still resolve the G6(imino) to C19(amino) cross peaks (E and E′), confirming the existence of an intact G6·C19 Watson–Crick base pair. However, it is difficult to unambiguously identify an NOE from the G6 imino proton to the H2 protons of any of the three bulged

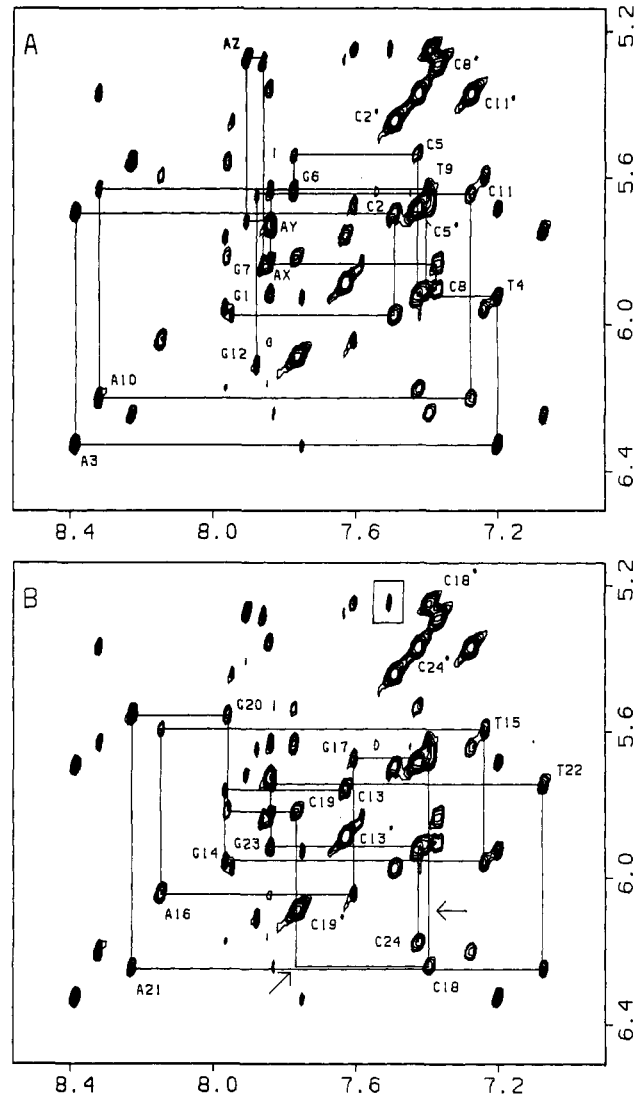

FIGURE 6: Expanded contour plot of the base to H1′ region of the NOESY experiment (250-ms mixing time) on the A_3-bulge duplex in D_2O buffer at 25 °C. Sequential distance connectivities are traced out for the bulge-containing strand (panel A) and partner strand (panel B) separately. Intraresidue base to H1′ cross peaks are labeled by residue. Asterisks indicate the H6–H5 cross peak for cytosine residues. The arrows in panel B indicate absent or weak NOEs for the C18–C19 base step across from the bulge site. The boxed peak in this panel is a cross-strand NOE between the Ay(H2) and the C18(H5) protons.

adenines in this molecule. Cross peak K in Figure 5 represents a probable NOE between the G6(imino) and Ax(H2) protons. However, the overlap with another guanine(imino) to adenine(H2) cross peak (peak L in Figure 5) makes absolute detection of this NOE difficult. On the basis of this result in H_2O, we can place the residues Az, and tentatively Ax, from the A_3-bulge duplex as stacked within the double helix. No cross peaks are seen to or from the Ay(H2) proton in this experiment. Table III lists the chemical shifts of all exchangeable and adenine H2 protons assigned for the A_3-bulge duplex.

Nonexchangeable Protons in the A_3-Bulge Duplex. An expanded contour plot of the base to H1′ region of the NOESY experiment (250-ms mixing time) for the A_3-bulge duplex in D_2O buffer at 25 °C is shown in Figure 6. Once again, sequential connectivities are traced out for the individual strands separately in panels A and B. For the most part, the results are similar to those seen for the A_2-bulge duplex. The protons from all three bulged adenines exhibit chemical shifts that lie further upfield than those of protons from other ad-

Table III: Exchangeable and A(H2) Proton Chemical Shifts of the A_3-Bulge Duplex in H_2O Buffer, pH 6.5, at 0 °C

	chemical shifts (ppm)				
base pair	H3	H1	NH_2b^a	NH_2e^b	H2
G1·C24			8.23	6.65	
C2·G23		12.85	8.47	6.61	
A3·T22	13.67				7.77
T4·A21	13.68				7.84
C5·G20		12.85	8.69	7.16	
G6·C19		12.87	8.73	7.30	
Ax					7.56
Ay					
Az					7.68
G7·C18		12.48	7.83	6.34	
C8·G17		12.70	8.14	6.58	
T9·A16	13.87				7.44
A10·T15	13.66				7.54
C11·G14		12.87	8.37	6.86	
G12·C13			8.16	7.11	

[a] Hydrogen-bonded cytosine amino protons. [b] Exposed cytosine amino protons.

enine residues. Sequential connectivities for the G6–Ax, Ay–Az, and Az–G7 base steps are visible in both the base to H1′ region (Figure 6A), as well as in the base to H2′,2″ region. On the opposite strand the sequential NOEs between C18 and C19 are absent in the H1′ (Figure 6B) and H2′,2″ region but are retained in the base to H3′ region (see Figure 4C).

We were unable to confirm the existence of any sequential NOEs between Ax and Ay, as the H8 protons from these two bases are overlapped in the NOESY spectrum (see Figure 6A). This redundancy could not be alleviated by adjusting the temperature of the sample. We therefore prepared an analogue of the A_3-bulge duplex in which the second adenine within the bulge loop, Ay, was replaced by an inosine residue. Inosine is a purine base that resembles both guanine, with a keto group in the 6 position, and adenine, with a nonexchangeable H2 proton. NMR studies of I·C bases incorporated into DNA (Boyd et al., 1990) indicate that the H8, H2, and imino protons of inosine resonate farther downfield than do similar protons on adenine or guanine residues. We therefore expected a large chemical shift difference between the H8 protons from the Ax and Iy residues within this AIA-bulge duplex. Unfortunately, the chemical shift difference between Ay(H8) and Iy(H8) at 25 °C is a mere 0.02 ppm. This was sufficient, however, to allow us to identify sequential NOEs for the Ax–Iy base step. Figure 7 shows comparative contour plots of part of the base to H2′,2″ regions of the NOESY spectra in D_2O buffer for the A_3-bulge duplex (panel A) and the AIA-bulge duplex (panel B). In Figure 7A, the overlap between Ax(H8) and Ay(H8) makes resolution of individual cross peaks impossible. In Figure 7B, the chemical shift difference between the Ax(H8) and Iy(H8) protons allows us to observe two new sequential NOEs, from the H2′ and H2″ protons of Ax to the H8 proton of Iy. These are designated by arrows in Figure 7B. The chemical shifts for most other protons, both within and outside the bulge loop region, are nearly identical from one duplex to the other. Thus it is fair to say that the AIA-bulge duplex resembles the A_3-bulge duplex quite well and that sequential connectivities for the Ax–Ay base step in the A_3-bulge duplex would be visible were it not for the degeneracy of the two H8 proton chemical shifts.

One additional NOE is seen in the A_3-bulge (and AIA-bulge) duplexes that was not observed in any of the other duplexes. This cross peaks is boxed in the upper right of Figure 6B. Inspection of the figure reveals that this cross peak maps to the C18(H5) proton in the ω_1 axis (vertical axis). A one-

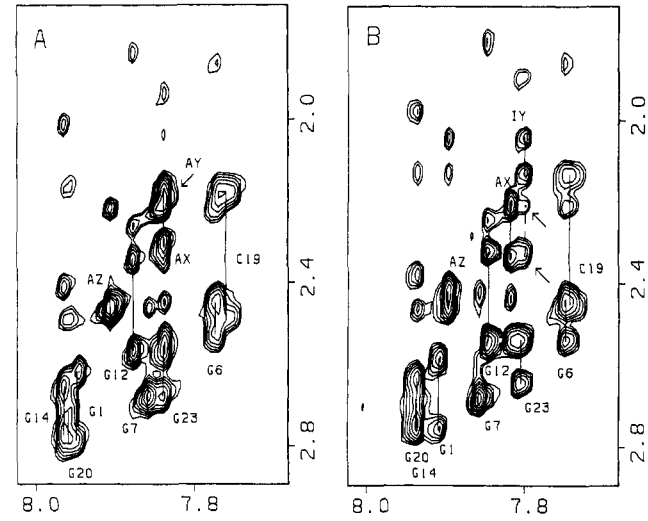

FIGURE 7: Expanded contour plots comparing identical regions of NOESY experiments in D_2O buffer at 25 °C on the A_3-bulge (panel A) and the AIA-bulge (panel B) duplexes. The region shown lies within the base to H2′,2″ portion of the spectra. Intraresidue NOEs for a variety of bases that fall within this region are indicated. In panel A, the overlap between the Ax(H8) and Ay(H8) protons makes resolution of individual cross peaks impossible. In panel B, the spectral resolution of the Ax(H8) and Iy(H8) protons allows for the observation of two sequential NOEs (connected by a dotted line and indicated with arrows) at this Ax–Iy base step.

dimensional inversion–recovery experiment showed that this cross peak originates from an adenine H2 proton in the ω_2 dimension. On the basis of the relative position of all adenine H2 protons in the spectra, we can assign this cross peak to the Ay residue within the bulge. Furthermore, in the AIA-bulge, this proton shows a strong NOE to the Iy(imino) proton in H_2O buffer. This unusual cross strand NOE between the Ay(H2) and C18(H5) protons establishes that Ay is also stacked within the double helix in the A_3-bulge duplex. On the basis of this information, as well as the data from the AIA-bulge duplex and from the A_3-bulge duplex in H_2O, we conclude that in the A_3-bulge molecule, each of the three bulged bases adopts an intrahelical conformation, stacking within the duplex. The chemical shifts of all nonexchangeable protons assigned in the A_3-bulge duplex are listed in Table IV.

Comparison of One-Dimensional Phosphorus Spectra. Figure 8 shows a comparison of the one-dimensional, proton-decoupled, phosphorus spectra of the control and bulge loop duplex molecules at 30 °C. The most striking aspect in the figure is the appearance of one downfield-shifted phosphorus resonance in each of the bulge loop duplexes. Interestingly, this resonance moves farther downfield as the size of the bulge loop increases. Gel migration assays have shown that for multiple-base bulge loops within duplex DNA, increases in the number of bases within the loop leads to parallel increases in the angle of bending (Bhattacharyya & Lilley, 1989; Hsieh & Griffith, 1989). Since ^{31}P chemical shifts of DNA are thought to be related to backbone conformation (Roongta et al., 1990), it is noteworthy that the position of a uniquely shifted phosphorus resonance in our duplexes moves farther downfield as the induced bend in the helical axis increases.

Assignment of Phosphorus Resonances in the A_3-Bulge Duplex. In order to determine the site of backbone perturbation in the bulge loop duplexes, we ran a proton-detected ^{31}P–^1H correlation experiment on the A_3-bulge duplex. A contour plot of the experiment is shown in Figure 9. For the downfield-shifted phosphorus resonance at −3.74 ppm, we see strong correlation peaks to the Az(H3′) and G7(H4′) protons.

Table IV: Chemical Shift Assignments for the A_3-Bulge Duplex in D_2O Buffer at 25 °C

	chemical shifts (ppm)							
base	H8/H6	H5/CH_3	H2	H1′	H2′	H2″	H3′	H4′
G1	7.94			5.97	2.62	2.79	4.85	4.24
C2	7.49	5.44		5.69	2.20	2.51	4.91	4.22
A3	8.38		7.75	6.32	2.75	2.99	5.06	4.46
T4	7.20	1.48		5.92	2.02	2.43	4.86	4.17
C5	7.42	5.68		5.53	1.87	2.23	4.79	4.05
G6	7.77			5.63	2.45	2.54	4.92	4.26
Ax	7.83		7.54	5.82	2.18	2.30	4.85	4.14
Ay	7.83		7.50	5.73	2.22	2.22	4.81	3.96
Az	7.90		7.63	5.28	2.46	2.46	4.81	4.19
G7	7.85			5.84	2.68	2.68	4.95	4.36
C8	7.37	5.29		5.90	2.02	2.45	4.70	4.21
T9	7.40	1.64		5.63	2.13	2.44	4.87	4.19
A10	8.31		7.54	6.20	2.71	2.85	5.03	4.43
C11	7.27	5.37		5.64	1.84	2.27	4.77	4.14
G12	7.87			6.11	2.57	2.34	4.64	4.15
C13	7.62	5.88		5.76	2.01	2.41	4.69	4.06
G14	7.96			5.96	2.65	2.77	4.96	4.36
T15	7.24	1.48		5.59	2.06	2.37	4.85	4.16
A16	8.14		7.45	6.04	2.68	2.86	5.03	4.39
G17	7.60			5.68	2.45	2.60	4.97	4.35
C18	7.39	5.25		6.24	2.03	2.20	4.81	4.29
C19	7.76	6.09		5.82	2.17	2.48	4.91	4.24
G20	7.96			5.59	2.72	2.79	4.99	4.30
A21	8.22		7.83	6.24	2.62	2.92	5.00	4.44
T22	7.07	1.39		5.74	1.93	2.34	4.84	4.12
G23	7.84			5.91	2.57	2.68	4.95	4.34
C24	7.42	5.37		6.17	2.18	2.18	4.48	4.05

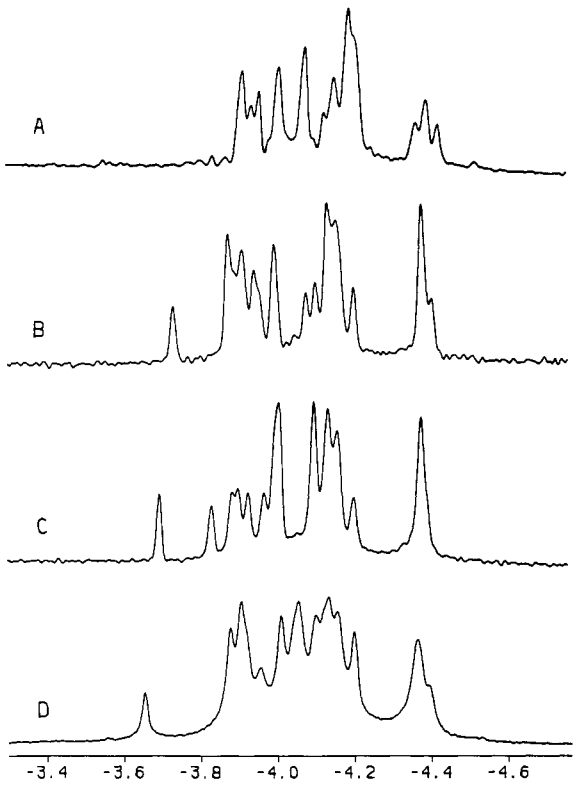

FIGURE 8: One-dimensional, proton-decoupled, phosphorus spectra of the control and bulge loop duplexes in D_2O buffer at 30 °C. (A) Control duplex. (B) A_1-bulge duplex. (C) A_2-bulge duplex. (D) A_3-bulge duplex.

We therefore can assign this phosphorus resonance to the internucleotide phosphate at the Az–G7 base step of the A_3-bulge duplex. Due to the density of cross peaks and the poor dispersion of the H3′ and H4′ protons, few of the other phosphorus resonances at or near the bulge loop site could be assigned. While it is probable that the backbone is perturbed at other base steps near the lesion, evidently none of these conformational features result in unusual phosphorus chemical shifts.

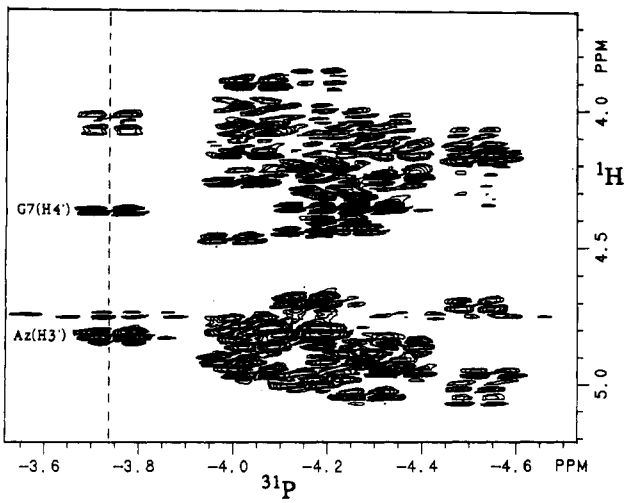

FIGURE 9: Contour plot of the proton-detected, phase-sensitive, ^1H–^{31}P correlation experiment of the A_3-bulge duplex in D_2O buffer at 25 °C. Positive and negative contours are shown. Cross peaks observed from the downfield-shifted phosphorus resonance at −3.74 ppm are labeled. These cross peaks enable us to assign this phosphorus resonance to the Az–G7 base step.

Discussion

Structural Features of Multiple-Base Bulge Loops in DNA. We have characterized the structural features of A, A-A, and A-A-A bulge loops within a DNA duplex by one- and two-dimensional NMR. We find that, for each duplex, all of the bulged adenines adopt intrahelical positions within the duplex. These results expand upon the prior observations regarding the intrahelical preference of singly-bulged purines in DNA. This preference evidently continues for bulges up to three bases in length. NMR studies on singly-bulged pyrimidine residues within duplex DNA have shown that the intrahelical stacking of these bulged bases is not assured under all conditions. Flanking sequence and even temperature can affect the transition between a stacked-in or a looped-out conformation for the bulged pyrimidine. It is therefore possible that multiple-pyrimidine bulge loops would exhibit conformational features different from those seen for our A_n-bulge duplexes. In some studies, T_n-bulge and U_n-bulge loops have been shown to cause less bending of the helix than do A_n-bulge loops of the same size (Bhattacharyya & Lilley, 1989; Tang & Draper, 1990).

We find that the presence of a two- or three-base bulge loop does not prevent the formation of Watson–Crick pairing in the flanking GC bases. In all of our bulge loop duplexes, both the G6·C19 and the G7·C18 base pairs are intact. It is unclear whether AT base pairs would be as resilient to the destabilization of a flanking multiple-base bulge loop. A recent study on the effects of flanking sequence on bending of DNA by bulged loops (Wang & Griffith, 1990) demonstrated that single-base bulges flanked by AT base pairs caused less gel retardation than did the same bulge flanked by GC pairs. It is possible that flanking base pair stability might have an effect on the degree of bending induced by bulge loops.

In this paper, we present general structural features of the A_2-bulge and A_3-bulge duplexes based on solution NMR observations. It is evident from our data that all of the bulged adenine residues in our duplexes adopt intrahelical positions. There is, however, little detailed information regarding the conformation of the bulged bases within the duplex. In the

A_3-bulge duplex, we do see one unusual NOE between the Ay(H2) and the C18(H5) protons. The observation of this cross-strand NOE is puzzling, since the H5 proton of cytosine lies in the major groove while the H2 proton of adenine is normally found in the minor groove. The Ay(H2)–C18(H5) NOE suggests that the bases within the bulge loop adopt an unusual conformation within the duplex. These bases might possibly be laterally shifted away from the helical axis.

Across from the bulge site, the C18–C19 base step exhibits an unusual set of sequential distance connectivities. The H3′ proton of C18 shows strong NOEs to both the H6 and H5 protons of C19 (Figure 4). All other sequential NOEs for this base step are absent or weak in the A_2-bulge and A_3-bulge duplexes. This finding demonstrates that while the two bases across from the bulge loop site are spatially separated, not all interproton distances within this step are increased. Most probably, there is a lateral aspect to the separation between C18 and C19.

We have attempted to derive a detailed, three-dimensional structure of both the A_2-bulge and A_3-bulge duplex using NOESY-derived proton–proton distance restraints as inputs for molecular dynamics simulations. We have succeeded in generating resonable structures in which all of the bulged adenines are stacked within the helix. However, we cannot reproducibly define a unique conformation within the bulge loop. In the A_2-bulge and A_3-bulge duplexes, we have little information regarding the distance between base protons within the bulge loop. Putative NOEs between the H8 or the H2 protons of the bulged residues are obscured by their proximity to the diagonal in the NOESY spectra. This situation is further exasperated by the overlap of the Ax(H8) and the Ay(H8) protons in the A_3-bulge duplex. The partial resolution of these resonances in the AIA-bulge duplex does not allow for accurate quantitation of NOESY cross peak volumes.

In order to overcome these difficulties regarding the poor spectral dispersion of base protons within A_n bulge loops, we have synthesized and studied an analogue of the A_3-bulge duplex which contains an A-T-A bulge loop. The large chemical shift differences among the base protons of adenine and thymine resulted in resolution of base to base NOEs within the loop. This in turn enabled us to determine distance restraints within the bulge loop that allowed us to characterize structural features of the bulge loop more reliably. We therefore defer further discussion of the detailed three-dimensional structure of bulge loops in DNA to the following paper in this issue, where we present the NMR results and structure determination of this ATA-bulge duplex in solution.

Our results for the A_2-bulge and A_3-bulge duplex disagree with an earlier model of multiple-base bulge loops (Bhattacharyya & Lilley, 1989). In this work, the authors studied A_n- and T_n-bulge loops, either three or five bases in length, with small molecular probes that specifically react with single-stranded nucleotides. The results of this study led the authors to conclude that most of the bases within these bulges were looped out into solution. Our results show that, for A_n-bulges up to three bases in length, all of the unpaired adenines stack within the helix. In the following paper in this issue on the solution structure of an ATA-bulge loop, we examine this discrepancy between the solution NMR and chemical modification data in more detail.

Proton Chemical Shift Trends for the A_n-Bulge Duplex Series. We have assigned most of the proton resonances for the A_n-bulge duplex series where n ranges from 0 to 3. These results are listed in the tables provided in the paper and the Supplementary Material. We have analyzed these results in order to determine the extent of conformational perturbation induced by the presence of a bulge loop defect. We find that chemical shift differences from the control sequence are greatest for the bases flanking the bulge loop and are minimal on proceeding more than two bases beyond the site of the loop. This result is represented quantitatively in Figure 10. For each of the bulge duplexes, we have plotted the average change in nonexchangeable proton chemical shifts, by residue, upon insertion of the bulged base(s) within the helix. The results for the two strands are shown separately in Figure 10, panels A and B. The most significant changes in chemical shift take place in residues that flank the bulge loop: G6 and G7 (also C5) on the bulge strand and C18 and C19 on the partner strand. The proton chemical shifts from residues more than two base steps away from the defect are practically indistinguishable from those of the control duplex.

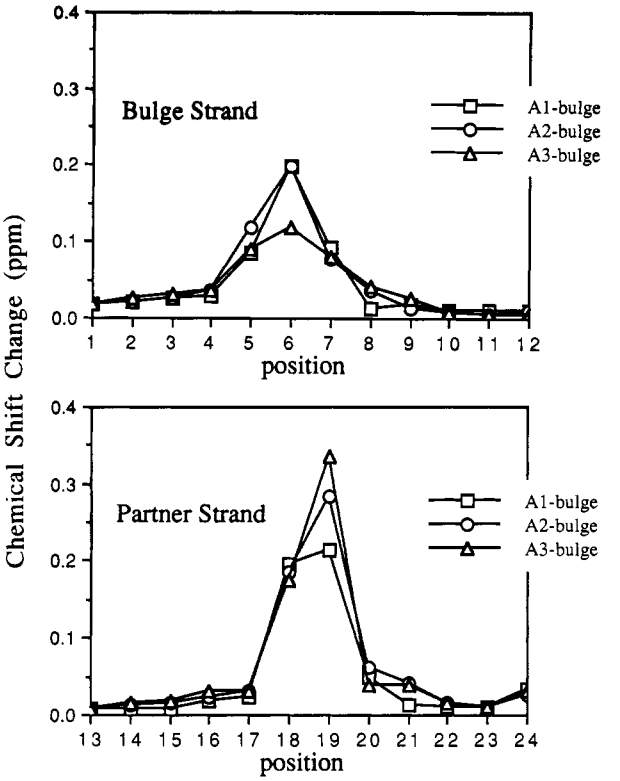

FIGURE 10: Plot of the nonexchangeable chemical shift differences, averaged by residue, between the control duplex and each of the bulge loop duplexes. The bulge-containing and partner strands are shown separately.

The data presented in Figure 10 suggest that the conformational change upon the insertion of a single adenine residue is much greater than any subsequent change upon the insertion of additional unpaired bases. This pattern was noted previously in the one-dimensional spectra of the different bulge duplexes in H_2O buffer. In fact, the mean chemical shift change for residue G6 in the A_3-bulge duplex is lower than that for the same residue in either the A_1-bulge or A_2-bulge duplexes. However, closer examination of individual proton chemical shifts reveals a more complex picture. The change in chemical shift versus the number of bases within the bulge loop is shown for various flanking base and sugar protons in Figure 11. Some proton resonances move downfield upon bulge loop insertion while others are relatively unaffected. Bidirectional patterns of chemical shift migration are also seen, such as for the H1′ proton of C19, which at first moves upfield in the A_1-bulge duplex and then shifts downfield in the A_2-bulge and A_3-bulge duplexes. The additive effect of additional bulged bases is clearly seen, however, in the chemical shift behavior

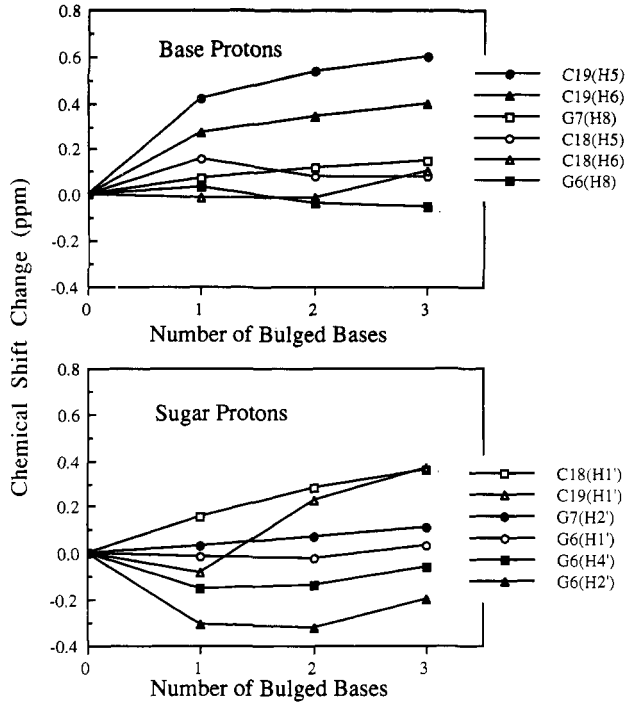

FIGURE 11: Plot of chemical shift differences (bulge loop duplex minus control duplex) versus number of bulged bases for various protons from residues flanking the bulge site. The additive effect of additional bases within the bulge loop can be seen for the H1′ proton of residue C18 and for the H6 and H5 protons of residue C19.

of the most prominently effected resonances, the H5 and H6 protons of C19, which resonate farther downfield as the bulge size increases. We have attributed the chemical shift changes in the C19 base protons to the disruption of base stacking between C18 and C19. These proton chemical shifts thus serve as physical markers of the progressively greater conformational effects of additional bases within bulge loops in DNA, as exhibited by the anomalous migration of bulge-containing duplexes in polyacrylamide gel electrophoresis.

It is difficult to examine similar trends in the chemical shifts of protons within the bulged adenine residues, as these bases have no counterparts in the control duplex. We do notice, however, a correspondence between the proton chemical shift values of residue Ay in the A_2-bulge duplex and those of residue Az in the A_3-bulge duplex. For example, the chemical shift of the H1′ proton of each of these residues falls quite far upfield in the NOESY spectra (compare Figure 3A with Figure 5A, or Table II with Table IV). A similar correspondence exists between the H2′, H2″, and H3′ protons from these two residues. Both of these residues are located at the 3′ end of the bulge loop in their respective duplexes. The similar magnetic environment experienced by these two residues suggests common conformational features at the 3′ end of the bulge loops in the A_2-bulge and A_3-bulge duplexes.

Phosphorus Chemical Shifts in the A_n-Bulge Series. In our series of A_n-bulge duplexes, we see a single phosphorus resonance located downfield from the main cluster of peaks. This phosphorus resonance moves farther downfield as the number of bases within the bulge loop increases. Given the effect that bulge loops have on the geometry of DNA duplexes, it is of interest to know where the backbone perturbations occur in these molecules. Previous NMR studies of single base purine bulges in duplex DNA have also demonstrated the appearance of a downfield-shifted phosphorus resonance (Patel et al., 1982; Roy et al., 1987; Woodson & Crothers, 1987; Kalnik et al., 1989a; Nikonowicz et al., 1989). For an adenine bulge within a -C-A*-G- sequence (the asterisk represents the bulged base), the downfield phosphorus resonance was shown to belong to the phosphate of the A*–G step of the molecule, on the 3′ side of the bulged adenine (Nikonowicz et al., 1989). Our results generalize this finding to bulge loops with multiple bases. For A_n bulges, the most downfield phosphorus resonance in bulge loop duplexes lies to the 3′ side of the last base within the loop. The correspondence in the proton chemical shifts of residue Ay in the A_2-bulge duplex and residue Az in the A_3-bulge duplex, both of which are at the 3′ terminus of the bulge loop, has already been noted. The unusual phosphorus chemical shift (assigned to the Az–G7 base step in the A_3-bulge duplex) is additional evidence of a common structural feature at the 3′ end of A_n bulge loops.

We note that the greater the number of bases within the loop, the greater the downfield shift of the unusual phosphorus resonance. This behavior was also seen in the base proton chemical shifts of residue C19. It is probable that the magnitude of these effects reach an upper limit, or even diminish, as one looks at larger bulge loops in DNA. This is undoubtably true of the bending phenomenon as well. It will be interesting to see whether these two characteristics of bulge loops in DNA—the magnitude of the induced bend in the helical axis and the unusual phosphorus and proton chemical shifts—continue to be correlated as additional bulge loops of different size and sequence are studied.

Conclusions

We have examined conformational features of one, two, and three bulged adenines within a dodecamer duplex by homonuclear and heteronuclear two-dimensional NMR spectroscopy. We find that even a three-base bulge loop can be easily accommodated within the DNA duplex. Watson–Crick hydrogen bonds for the GC base pairs flanking the bulge loop remain intact for each of the bulged duplexes studied. All bulged residues in our sequences adopt intrahelical positions, stacking within the helix. This contradicts an earlier model (Bhattacharyya & Lilley, 1989) of the conformation of multiple-base bulge loops in DNA.

The insertion of two or three unpaired bases into the DNA helix is accompanied by the disruption of the base stacking across from the bulge site on the opposite strand. The A_2-bulge and A_3-bulge duplexes exhibit identical proton chemical shift trends at the 3′ end of the bulge loop. An unusual phosphorus chemical shift in the A_3-bulge duplex is also localized to the base step at the 3′ end of the bulge. Comparison of proton and phosphorus chemical shifts for the different bulge loop duplexes indicate that additional bases within the bulge loop can have an additive effect on the structural perturbations caused by bulge loops in DNA, in agreement with gel mobility studies of multiple-base bulge loops.

This study demonstrates the applicability of high-resolution NMR spectroscopy toward the characterization of bending of DNA induced by the bulge loop defect. This process is advanced further in the following paper in this issue in which detailed structural features of a trinucleotide A-T-A bulge loop within a DNA duplex are presented.

Supplementary Material Available

Four tables listing the proton chemical shift assignments of the control duplex and the A_1-bulge duplex in H_2O and D_2O and two figures showing expanded contour plots of the base to H1′ region of the NOESY spectra of the control duplex and the A_1-bulge duplex in D_2O buffer at 25 °C (9 pages). Ordering information is given on any current masthead page.

REFERENCES

Bhattacharyya, A., & Lilley, D. M. J. (1989) *Nucleic Acids Res. 17*, 6821–6840.

Bhattacharyya, A., Murchie, A. I. H., & Lilley, D. M. J. (1990) *Nature 343*, 484–487.

Boyd, F. L., Stewart, D., Remers, W. A., Barkley, M. D., & Hurley, L. H. (1990) *Biochemistry 29*, 2387–2403.

Gutell, R. R., & Fox, G. E. (1988) *Nucleic Acids Res. 16*, r175–r270.

Hare, D. R., Wemmer, D. E., Chou, S. H., Drobny, G., & Reid, B. R. (1983) *J. Mol. Biol. 171*, 319–336.

Hare, D. R., Shapiro, L., & Patel, D. J. (1986) *Biochemistry 25*, 7456–7464.

Hsieh, C.-H., & Griffith, J. D. (1989) *Proc. Natl. Acad. Sci. U.S.A. 86*, 4833–4837.

Joshua-Tor, L., Rabinovich, D., Hope, H., Frolow, F., Appella, E., & Sussman, J. L. (1988) *Nature 334*, 82–84.

Joshua-Tor, L., Frolow, F., Appella, E., Hope, H., Rabinovich, D., & Sussman, J. L. (1992) *J. Mol. Biol.* (in press).

Kalnik, M. W., Norman, D. G., Swann, P. F., & Patel, D. J. (1989a) *J. Biol. Chem. 264*, 3702–3712.

Kalnik, M. W., Norman, D. G., Zagorski, M. G., Swann, P. F., & Patel, D. J. (1989b) *Biochemistry 28*, 294–303.

Kalnik, M. W., Norman, D. G., Li, B. F., Swann, P. F., & Patel, D. J. (1990) *J. Biol. Chem. 265*, 636–647.

Live, D., Davis, D. G., Agosta, W. C., & Cowburn, D. (1984) *J. Am. Chem. Soc. 106*, 1939–1941.

Miller, M., Harrison, R. W., Wlodawer, A., Appella, E., & Sussman, J. L. (1988) *Nature 334*, 85–86.

Morden, K. M., Chu, Y. G., Martin, F. H., & Tinoco, I., Jr. (1983) *Biochemistry 22*, 5557–5563.

Morden, K. M., Gunn, B. M., & Maskos, K. (1990) *Biochemistry 29*, 8835–8845.

Nelson, J. W., & Tinoco, I. (1985) *Biochemistry 24*, 6416–6421.

Nikonowicz, E., Roongta, V., Jones, J. R., & Gorenstein, D. G. (1989) *Biochemistry 28*, 8714–8725.

Nikonowicz, E. P., Meadows, R. P., & Gorenstein, D. G. (1990) *Biochemistry 29*, 4193–4204.

Patel, D. J., Kozlowski, S. A., Marky, L. A., Rice, J. A., Broka, C., Itakura, K., & Breslauer, K. J. (1982) *Biochemistry 21*, 445–451.

Peattie, D. A., Douthwaite, S., Garrett, R. A., & Noller, H. F. (1981) *Proc. Natl. Acad. Sci. U.S.A. 78*, 7331–7335.

Plateau, P., & Gueron, M. (1982) *J. Am. Chem. Soc. 104*, 7310–7311.

Rice, J. A., & Crothers, D. M. (1989) *Biochemistry 28*, 4512–4516.

Romaniuk, P. J., Lowary, P., Huey-Nan, W., Stormo, G., & Uhlenbeck, O. C. (1987) *Biochemistry 26*, 1563–1568.

Roongta, V. A., Jones, C. R., & Gorenstein, D. G. (1990) *Biochemistry 29*, 5245–5258.

Roy, S., Sklenar, V., Appella, E., & Cohen, J. S. (1987) *Biopolymers 26*, 2041–2052.

Sklenar, V., & Bax, A. (1987) *J. Am. Chem. Soc. 109*, 7526–7528.

Sklenar, V., Miyashiro, H., Zon, G., Miles, H. T., & Bax, A. (1986) *FEBS Lett. 208*, 94–98.

States, D. J., Haberkorn, R. A., & Ruben, D. J. (1982) *J. Magn. Reson. 48*, 286–292.

Streisinger, G., Okada, Y., Emrich, J., Newton, J., Tsugeta, A., Terzaghi, E., & Inouye, M. (1966) *Cold Spring Harbor Symp. Quant. Biol. 31*, 77–84.

Tang, R. S., & Draper, D. E. (1990) *Biochemistry 29*, 5232–5237.

van den Hoogen, Y. T., van Beuzekon, A. A., de Vroom, E., van der Marel, G. A., van Boom, J. A., & Altona, C. (1988a) *Nucleic Acids Res. 16*, 5013–5030.

van den Hoogen, Y. T., van Beuzekon, A. A., van den Elst, H., van der Marel, G. A., van Boom, J. H., & Altona, C. (1988b) *Nucleic Acids Res. 16*, 2971–2986.

Wang, Y.-H., & Griffith, J. (1991) *Biochemistry 30*, 1358–1363.

Weeks, K. M., Ampe, C., Schultz, S. C., Steitz, T. A., & Crothers, D. M. (1990) *Science 249*, 1281–1285.

White, S. A., & Draper, D. E. (1987) *Nucleic Acids Res. 15*, 4049–4064.

Wolters, J., & Erdmann, V. A. (1988) *Nucleic Acids Res. 16*, r1–r70.

Woodson, S. A., & Crothers, D. M. (1988) *Biochemistry 27*, 3130–3141.

Wüthrich, K. (1986) *NMR of Proteins and Nucleic Acids*, John Wiley & Sons, New York.

Yip, P., & Case, D. (1989) *J. Magn. Reson. 83*, 643–648.